Physics Open 17 (2023) 100164

Contents lists available at ScienceDirect

Physics Open

journal homepage: www.elsevier.com/locate/physo

Wave packet tunneling and imaginary wave vector dispersion

Walter Unglaub *, A.F.J. Levi

Department of Electrical and Computer Engineering, University of Southern California, Los Angeles, CA 90089-2533, USA

ARTICLE INFO

Handling Editor: Matteo Paris

Keywords:
Wave packet tunneling
Single-electron tunneling
Imaginary wave vector dispersion
Tight-binding model

ABSTRACT

Dispersion associated with the complex band structure of a periodic potential can be used to explain single-electron wave packet tunneling through a finite-sized tunnel barrier. The imaginary k-space dispersion in a tunnel barrier may be viewed as a filter that controls the arrival time, shape, and group velocity of a transmitted wave packet. This k-space filter can be designed to increase or decrease the group velocity of the transmitted pulse and a transmitted peak-pulse probability arrival time can be engineered to occur before or after that of an electron wave packet propagating in the absence of the tunnel barrier.

1. Introduction

Single-electron wave packet dynamics on a lattice is of both fundamental and practical interest. For example, basic questions associated with tunneling can be addressed by studying the collision of a wave packet with a tunnel barrier [1–3]. At the same time, emerging applications in nano-scale solid-state electronic devices can benefit from better understanding of electron transport and tunneling phenomena [4,5].

While the role of energy eigenstate dispersion in determining the behavior of a propagating single-electron wave packet comprised of states with real wave vector k is well understood [6,7], less is known about the dispersion of imaginary wave vectors and its influence on wave packet tunneling.

An example of band structure is the electron energy dispersion, ϵ_k, that occurs due to the Coulomb potential of single identical-atom occupancy of static lattice sites in a crystal of infinite extent. Complex band structure arises because the wave vectors appearing in the electron dispersion can be pure-real, corresponding to propagating states, or have an imaginary component, corresponding to localized non-propagating states. We show that the dispersion properties of electron motion in such periodic potentials can be used as a guide to explain the behavior of wave packet scattering at finite-sized tunnel barriers formed on a lattice.

In the following, electron wave packet dynamics at a tunnel barrier is studied using a tight-binding model. It is found that the imaginary k-space solutions to Schrödinger's equation in the tunnel barrier can be controlled and used as a filter to determine the shape, average arrival time, and group velocity of a single-electron transmitted pulse.

2. Electron propagation on a lattice

Electron eigenenergy dispersion, ϵ_k, as a function of wave vector k in the presence of a periodic Coulomb potential can be very different from the quadratic dispersion of free-space for which $\epsilon_k = \hbar^2 k^2/2m_0$, where m_0 is the bare electron mass. A lattice consisting of integer N atoms with nearest-neighbor separation L and periodic boundary conditions has electron energy eigenstates that may be modeled using a tight-binding approximation. If the energy associated with localized electron motion from one lattice site to a nearest-neighbor lattice site is t_h then, for a one-dimensional (1D) lattice in the $N \to \infty$ limit, there is a cosine dispersion relation, $\epsilon_k = -2t_h \cos(kL)$, with real electron wave vector $-\pi/L < k \leq \pi/L$. In this case each identical atom is assumed to have an electron s-orbital. When $|\epsilon_k| > 2t_h$, there are also solutions for which electron wave vector has an imaginary component. The dispersion in energy eigenvalues, ϵ_k, that exist as a function of real and imaginary wave vector values in the $N \to \infty$ limit is the complex band structure [8]. Electron states with real k can propagate and states with an imaginary component in k do not propagate and are localized in space.

For a single cosine band, approximately quadratic dispersion in ϵ_k as a function of real propagating k-states near the band minimum causes the standard deviation of a Gaussian wave packet probability density describing a low energy electron to broaden spatially as a function of time, t, such that $\Delta x(t) = \sqrt{\sigma_x^2 + (\omega'' t/2\sigma_x)^2}$, where σ_x is the initial standard deviation of the pulse, $\omega'' = \mathrm{d}^2\omega/\mathrm{d}k^2$, and $\epsilon_k = \hbar\omega(k)$. For the quadratic dispersion being considered, $\omega'' = \hbar/m_e^*$, where m_e^* is an effective electron mass. In this case, the leading edge of a propagating time-evolved Gaussian wave packet pulse contains higher

* Corresponding author.
E-mail address: unglaub@usc.edu (W. Unglaub).

https://doi.org/10.1016/j.physo.2023.100164
Received 24 June 2023; Accepted 26 June 2023
Available online 4 July 2023

spatial frequencies with higher energy components than the trailing edge.

To numerically simulate the time evolution of a single-electron wave packet on a finite 1D lattice with a tunnel barrier, we utilize the site representation for single-electron occupation at lattice position x_j, described by the basis state $|j\rangle$. Electron hopping occurs via the creation ($\hat{c}_j^\dagger$) and annihilation ($\hat{c}_j$) operators for the jth site, with $|0\rangle$ denoting the vacuum state such that $\hat{c}_j|0\rangle = 0$ and $\hat{c}_j^\dagger|0\rangle = |j\rangle$ corresponds to a single electron occupying the lattice site at position x_j. This is shown schematically in Fig. 1.

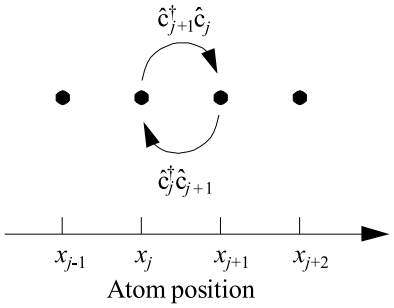

Fig. 1. Real-space nearest-neighbor electron hopping using the site representation on a 1D lattice.

The system requires defining the Hamiltonian $\hat{H}$ and performing numerical diagonalization to extract the system eigenvalues (see Appendix A). The Hamiltonian includes a kinetic energy term $\hat{T}$ which describes nearest-neighbor hopping and a potential energy $\hat{V}$ consisting of the real onsite values U_j. The total Hamiltonian is given by

$$\begin{aligned}\hat{H} &= \hat{T} + \hat{V} \\ &= -t_h \sum_{j=1}^{N} \left(\hat{c}_j^\dagger \hat{c}_{j+1} + \hat{c}_{j+1}^\dagger \hat{c}_j \right) + \sum_{j\in\mathcal{J}} U_j \hat{c}_j^\dagger \hat{c}_j,\end{aligned} \tag{1}$$

where t_h represents the energy for the electron to hop from one atomic site to a nearest-neighboring site (see Appendix B to find t_h for a given m_e^*). Periodic boundary conditions are applied. In the following, we explore tunnel barriers such that $U_j = V_B$ on a discrete number of lattice sites $j \in \mathcal{J}$ within the position range $x_j = [0, L_B]$, where L_B is the barrier thickness, and $U_j = 0$ elsewhere.

To define the initial state vector in terms of the site basis states $|j\rangle$, we must first explicitly define the value of the wave function amplitudes at each lattice site, x_j. This is done by taking the wave function describing an electron at time $t = 0$ consisting of a plane wave with momentum $\hbar k_0$ in the x-direction modulated by a Gaussian spatial function and then calculating an initial amplitude value $\psi_0(x_j, t = 0)$ for each site located at position x_j. The initial Gaussian wave function is

$$\psi\,(x, t = 0) = \left(\frac{1}{2\pi\sigma_x^2} \right)^{1/4} e^{ik_0 x} e^{-\frac{x^2}{4\sigma_x^2}} \tag{2}$$

with mean position $x_0 = 0$ at time $t = 0$. A measure of the spatial spread of the wave packet is the standard deviation σ_x.

In addition, we wish to ensure that no part of the wave packet is transmitted with energy greater than the barrier. This is achieved by restricting the highest wave vector value (and therefore the highest energy component) so that it corresponds to *less* than the onsite barrier energy V_B. Doing so guarantees that the pulse is transmitted via tunneling alone, thereby avoiding the Hartman effect in which a portion of electron probability can be transmitted over the top of the barrier [9]. Such predistortion of the wave packet is performed by applying a raised cosine filter to yield a non-Gaussian wave packet $\psi(x_j, t = 0)$, which we use as the initial incoming pulse. The raised cosine bounds wave packet energy components to values between E_{min} and E_{max}. See Appendix C.

The state vector for the initial wave function can then be written as a superposition of all basis states with corresponding amplitudes in real space,

$$|\psi(0)\rangle = \sum_{j=1}^{N} \psi(x_j, t = 0)|j\rangle. \tag{3}$$

In the special case where $V_B = 0$, the eigenstates can be described analytically as

$$|k\rangle = \frac{1}{\sqrt{N}} \sum_{j=1}^{N} e^{ikx_j} \hat{c}_j^\dagger |0\rangle, \tag{4}$$

with corresponding discrete energy eigenvalues $\epsilon_k = -2t_h \cos(kL)$, where k is real and L is the lattice spacing. There are also solutions for which k is pure imaginary.

The general eigenstates of the system may be obtained via matrix diagonalization and can be written as

$$|n\rangle = \sum_{j=1}^{N} a_j^{(n)} \hat{c}_j^\dagger |0\rangle = \sum_{j=1}^{N} a_j^{(n)} |j\rangle, \tag{5}$$

where $a_j^{(n)}$ are the eigenvector coefficients for the nth eigenstate with corresponding eigenvalue ϵ_n. The wave packet can then be unitary evolved to obtain the time-dependent state

$$|\psi(t)\rangle = \sum_{n=1}^{N} |n\rangle\langle n|\psi(0)\rangle e^{-i\epsilon_n t/\hbar}. \tag{6}$$

The time-dependent expression for the amplitude on each lattice site may be obtained by evaluating $\langle j|\psi(t)\rangle$,

$$\psi(x_j, t) = \sum_{n=1}^{N} a_j^{(n)} \langle n|\psi(0)\rangle e^{-i\epsilon_n t/\hbar}, \tag{7}$$

where $a_j^{(n)}$ represents the jth element of the nth eigenvector and $\langle n|\psi(0)\rangle = \sum_j [a_j^{(n)}]^* \psi(x_j, 0)$, in which $[a_j^{(n)}]^*$ represents the complex conjugate of eigenvector component $a_j^{(n)}$.

3. Wave packet dynamics at a tunnel barrier

An electron described by a single-peaked wave packet initially propagating in an electrode and incident on a tunnel barrier has, in general, a probability of being transmitted and reflected. If this electron of expectation energy E_0 is moving from left-to-right in the x-direction and is incident on a tunnel barrier of thickness L_B consisting of a discreet number of lattice sites with onsite energy V_B and $E < V_B$, it can tunnel and subsequently propagate as a pulse and be detected at some position to the right of the barrier.

As an initial step toward understanding the electron states involved, Fig. 2(a) shows a propagating electron state of energy E_0 as a dot in the real nearest-neighbor tight-binding cosine band of the electrode. In Fig. 2(b) the cosine band is shifted up in energy relative to (a) to represent the states associated with a tunnel barrier of energy V_B. An electron of energy E_0 and corresponding wave vector k_0 in the electrode that is incident on the tunnel barrier may be viewed as being able to tunnel via the pure imaginary k-state (dot) in the imaginary part of the complex band structure indicated in Fig. 2(b) (red dash curve).

3.1. High-pass k-space filter in a tunnel barrier

Fig. 3(a) illustrates an electron wave packet propagating on a lattice with zero onsite energy (upper sketch) and incident on a tunnel barrier with onsite energy V_B (lower sketch). Fig. 3(b) shows the result of solving pulse propagating on a lattice in the nearest-neighbor tight-binding approximation with and without a tunnel barrier. Note the use of a $\log_{10}$ scale so that the probability, $|\psi|^2$, of measuring the transmitted electron as a function of time with and without the tunnel barrier may be seen on the same plot. The numerical solution shows that the peak of an electron wave packet that has tunneled, and is measured in the electrode at some fixed position, x_R, far to the right

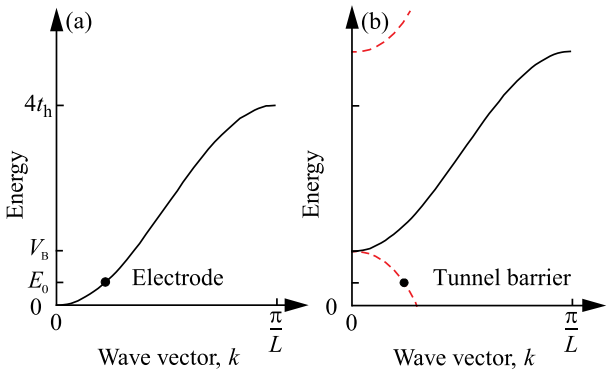

Fig. 2. (a) A propagating electron state (dot) of energy E_0 in the real nearest-neighbor tight-binding cosine band of the electrode (black curve). (b) Cosine band shifted up in energy relative to (a) to form a tunnel barrier of energy V_B. An electron of energy E_0 and corresponding wave vector k_0 incident on the barrier may be viewed as tunneling via the pure imaginary k-state (dot) in the band structure (red dash curve). (For interpretation of the references to color in this figure legend, the reader is referred to the web version of this article.)

of a tunnel barrier, can arrive at time t_p *before* the peak of the electron wave packet propagating in the absence of the barrier.

In a semiconductor heterostructure lattice, the k-space filter action of tunneling through a single barrier is related to, and hence may be viewed as controlled by, complex band structure. Pure imaginary wave vectors of magnitude κ in a semiconductor band gap determine probability amplitude attenuation of the pulse wave vector components that tunnel. Electron tunneling can be exponentially sensitive to imaginary band structure since, for an almost opaque barrier of thickness L_B, tunneling probability amplitude scales as $e^{-\kappa L_B}$.

In Fig. 3(b) the value of $t_p = 0.14$ ps, wave packet expectation energy is $E_0 = 0.15$ eV, onsite barrier energy is $V_B = 0.35$ eV, and barrier thickness is $L_B = 15$ nm.

In this case, for an incident wave packet with expectation energy $E_0 < V_B$, electron tunneling acts as a *high-pass filter* of plane-wave pulse components with momentum $\hbar k$. Higher energy components at the leading edge of the incident pulse have greater probability of tunneling. The transmitted pulse is distorted relative to the incident wave packet, contains time-independent k-states with amplitudes that peak at a value $k' > k_0$, and the *group velocity of the transmitted pulse is greater than that of the incident pulse*. This filtering in k-space, in which the magnitude of the fast Fourier transform (FFT) of $\psi(x > L_B)$ is plotted as a function of wave vector k, is illustrated in Fig. 4(a) for different values of barrier thickness, L_B. The numerical approach used for computing the FFT of the transmitted pulse is detailed in Appendix D. As shown in Fig. 4(b), for an incident pulse with fixed k_0 the group velocity, v_g, of the transmitted pulse *increases* with increasing σ_k and increasing L_B. Both the standard deviation of an incident real-space wave packet and tunnel barrier thickness may be used to control group velocity of the transmitted pulse.

Fig. 5(a) shows the calculated spatio-temporal plot of $|\psi(x,t)|^2$ for an electron wave packet propagating on a lattice with constant onsite energy and Fig. 5(b) shows the case when there is a tunnel barrier. The solid sloped lines are at the peak of the incident and transmitted pulses. These lines have different slopes because the group velocity of the incident and transmitted pulse is not the same. The offset at the tunnel barrier is due to the k-space filtering effect and its impact on $|\psi(x,t)|^2$ is shown in more detail in Fig. 6. The leading edge of the incident pulse has higher energy components and so greater probability of tunneling. Also evident is the fact that the reflected portion of the single-electron pulse interferes with itself and strongly influences the behavior of $|\psi(x,t)|^2$ near the barrier during the collision.

Fig. 7 is a plot of spatial probability distribution $|\psi(x,t_m)|^2$ at a specific time $t_m = 0.58$ ps. Note the use of a $\log_{10}$ scale makes

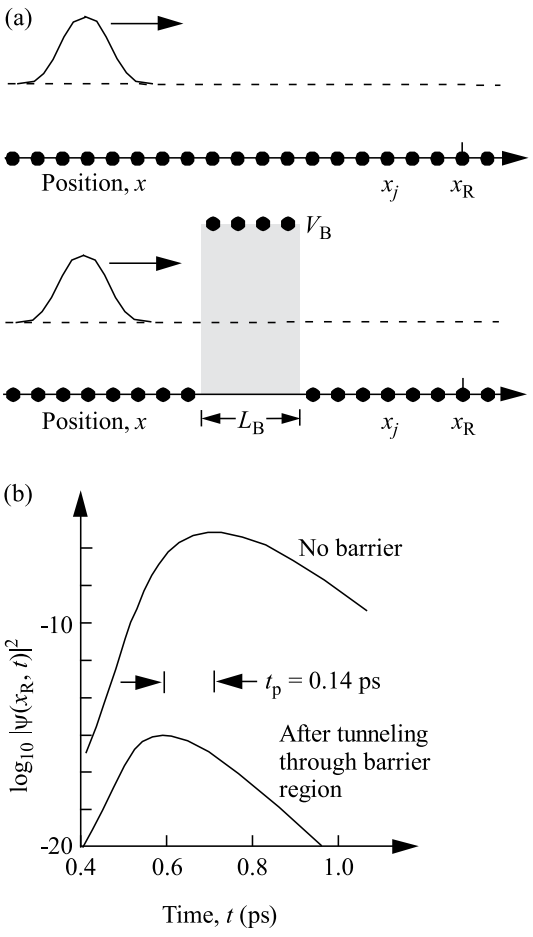

Fig. 3. (a) An electron wave packet propagating on a lattice with zero onsite energy (upper sketch) and incident on a tunnel barrier with onsite energy V_B (lower sketch). Measurement at fixed position, x_R, is far to the right of the tunnel barrier. (b) Calculated probability of measuring the transmitted electron at x_R as a function of time with and without a tunnel barrier. In the presence of a tunnel barrier with onsite energy V_B and thickness L_B, the electron with expectation energy $E_0 < V_B$ has a peak detection probability that in this case occurs at time $t_p = 0.14$ ps *before* the peak for an electron propagating in the absence of the tunnel barrier. Parameters are $L = 0.5$ nm, $t_h = 2.177$ eV, $\sigma_k = 0.07$ nm^{-1}, $\sigma_x = 7.14$ nm, $k_0 = 0.527$ nm^{-1}, $L_B = 15$ nm, $E_{min} = 34$ meV, $E_0 = 150$ meV, $E_{max} = 346$ meV, $V_B = 350$ meV, $v_{g,0} = 8.6 \times 10^5$ m s^{-1}, $x_0 = -400$ nm, $x_R = 407.5$ nm.

apparent the self-interference from particle reflection at the barrier and exponential suppression of particle transmission tunnel probability.

3.2. Low-pass k-space filter in a tunnel barrier

Fig. 2 is a convenient way to illustrate the role that dispersion of the pure imaginary states in the tunnel barrier plays to create an effective high-pass k-space filter for a transmitted single-electron pulse. Relative to the incident pulse, this filter action changes the shape of the transmitted pulse, it increases the group velocity of the transmitted pulse, and results in a transmitted peak-pulse arrival time that occurs before that of an electron wave packet propagating in the absence of the barrier.

We now show how to access different dispersion in the tunnel barrier and create a low-pass k-space filter whose effect is to decrease the group velocity of the transmitted pulse and have a transmitted peak-pulse arrival time occur after that of an electron wave packet propagating in the absence of the barrier. Again, we adopt the simplest approach and only use a single nearest-neighbor tight-binding cosine band.

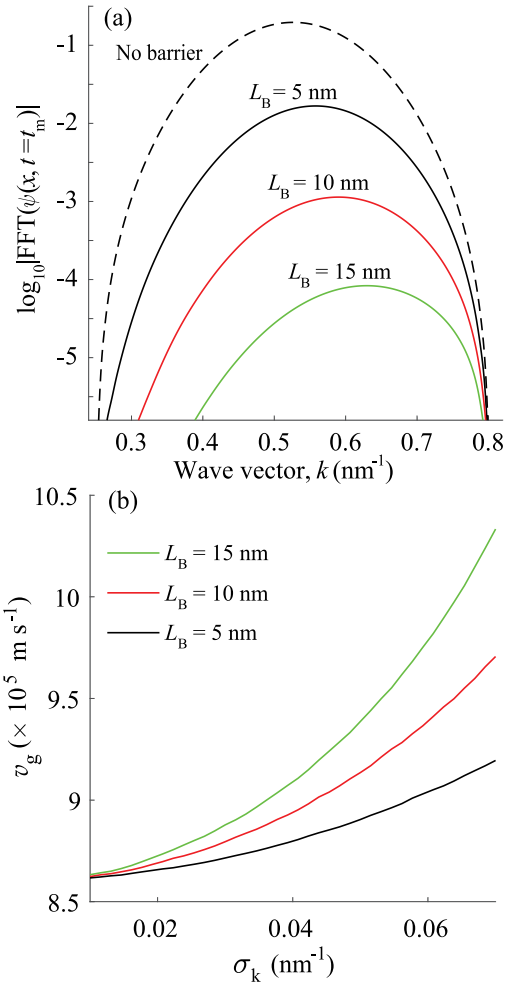

Fig. 4. (a) An incident electron wave packet of expectation energy E_0 has a distribution of k-space amplitudes with a standard deviation $\sigma_k = 0.07$ nm^{-1} centered on wave vector $k_0 = 0.527$ nm^{-1}. Because higher energy components of the wave packet have an enhanced probability of tunneling, the tunnel barrier of thickness L_B acts as a high-pass filter for wave vector amplitudes. The transmitted pulse measured at time $t_m > 0.78$ ps is distorted relative to the incident pulse, contains k-states with amplitudes that peak at a value $k' > k_0$, and has a group velocity that is greater than that of the incident pulse. For barrier thicknesses $L_B = 5$, 10, and 15 nm, $k' = 0.558$, 0.590, and 0.630 nm^{-1} respectively. (b) Transmitted pulse group velocity depends on σ_k and L_B. Parameters are as in Fig. 3.

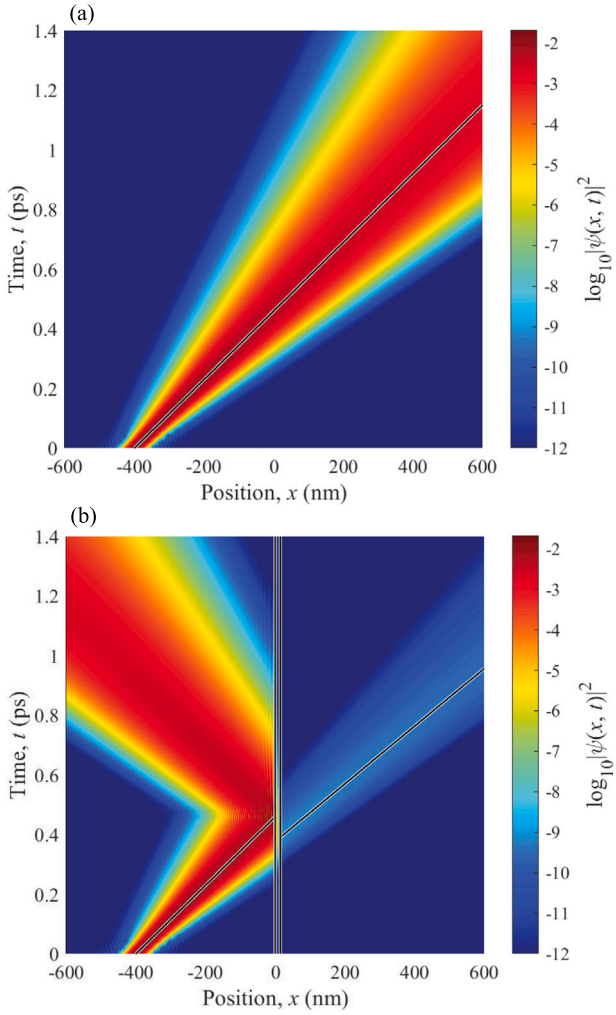

Fig. 5. (a) Spatio-temporal plot of a Gaussian pulse describing electron probability $|\psi(x,t)|^2$ propagating on a lattice with constant onsite energy. Peak pulse position is shown as a line whose slope is inversely proportional to group velocity, v_g. (b) Electron pulse propagating on a lattice incident on a barrier with onsite energy V_B. Vertical lines indicate left and right boundaries of the tunnel barrier. After transmission through the barrier the electron wave packet has a group velocity that is greater than that of the pulse propagating in the absence of the barrier. The peak in the attenuated transmitted pulse arrives *before* the peak of the pulse propagating in the absence of the tunnel barrier. Parameters are as in Fig. 3.

Fig. 8(a) shows a propagating electron state of energy E_0 as a dot in the real nearest-neighbor tight-binding cosine band of the electrode. In Fig. 8(b) the cosine band is shifted down in energy relative to (a) to access states associated with a tunnel barrier. An electron of energy E_0 in the electrode that is incident on the barrier may be viewed as being able to tunnel via the k-state (dot) in the complex part of the band structure indicated in Fig. 8(b) (red dash curve). Notice that the slope and curvature of the imaginary band in the barrier near electron energy E_0 has the opposite sign compared to the case shown in Fig. 2. It is this difference in imaginary dispersion that changes transmitted electron-pulse behavior through the tunnel barrier from that of an effective high-pass filter to a low-pass filter in k-space.

While normal dispersion in the electrode ensures high energy components of the incident pulse arrive at the tunnel barrier first, when electron tunneling acts as a *low-pass filter* of plane-wave pulse components with momentum $\hbar k$, lower energy components of the incident pulse can have greater probability of tunneling. As a consequence, the transmitted pulse is distorted relative to the incident wave packet, contains k-states with amplitudes that peak at a value $k' < k_0$, and the *group velocity of the transmitted pulse is less than that of the incident pulse*. This filtering in k-space is illustrated in Fig. 9(a). The change in k' with increase in L_B is not as rapid as in Fig. 4(a) because the low-pass k-space filter of the tunnel barrier must overcome the dispersion of the incident pulse whose leading edge contains high spatial frequencies with correspondingly high values of momentum.

As shown in Fig. 9(b), for an incident pulse with fixed k_0 the group velocity v_g of the transmitted pulse *decreases* with increasing σ_k and increasing L_B. This again demonstrates that changing the standard deviation of an incident particle described by a real-space wave-packet of energy expectation value E_0 or changing the barrier thickness controls the group velocity of the transmitted pulse.

Fig. 10(a) shows the spatio-temporal plot of $|\psi(x,t)|^2$ for an electron wave packet incident on a tunnel barrier. The solid sloped lines are at the peak of the incident and transmitted pulses. The lines have different slopes because the group velocity of the incident pulse is greater than that of the transmitted pulse. The offset at the tunnel barrier is due to the k-space filtering effect in the tunnel barrier and its impact on $|\psi(x,t)|^2$ is shown in more detail in Fig. 10(b). The

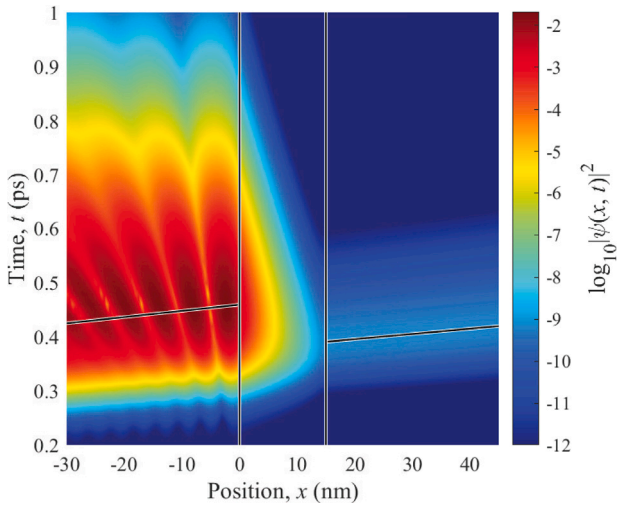

Fig. 6. Detail of Fig. 5(b). The leading edge of the incident pulse has higher energy components and so greater probability of tunneling. Vertical lines indicate the left and right boundaries of the tunnel barrier.

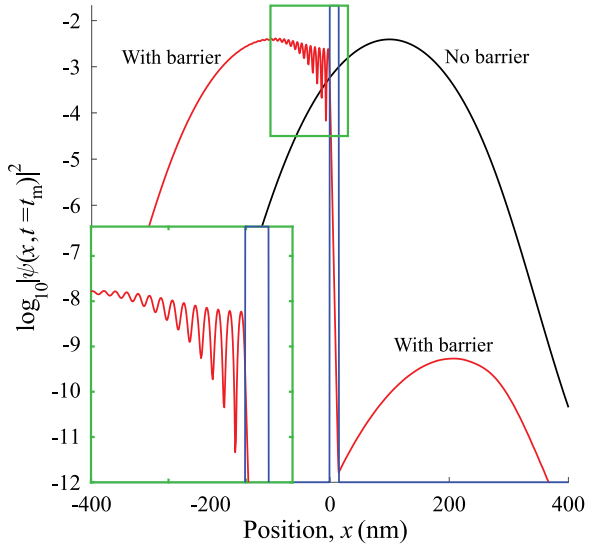

Fig. 7. Calculated electron probability $|\psi(x,t_m)|^2$ at time $t_m = 0.58$ ps with zero onsite energy and in the presence of a tunnel barrier with onsite energy $V_B = 0.35$ eV. Vertical lines indicate the left and right boundaries of the barrier. Detail of self-interference due to reflection from the tunnel barrier is shown in the inset. The transmitted electron wave packet group velocity is greater than that of the pulse propagating in the absence of the barrier. The peak in the attenuated transmitted pulse describing an electron that has tunneled through the barrier arrives a time t_p *before* the peak of the pulse propagating in the absence of the barrier. Parameters are as in Fig. 3.

peak in the attenuated transmitted pulse arrives *after* the peak of the pulse probability propagating in the absence of the tunnel barrier. The reflected portion of the single-electron pulse interferes with itself and strongly influences the behavior of $|\psi(x,t)|^2$ near the barrier during the collision.

4. Discussion

The difference in time that a particle spends interacting with and without a local potential is called the collision lifetime [10]. However, it seems that this is not helpful in explaining single-electron dynamics at a tunnel barrier. Rather, the behavior of single-electron wave-packet tunneling is most easily explained if the tunnel barrier is viewed as a k-space filter.

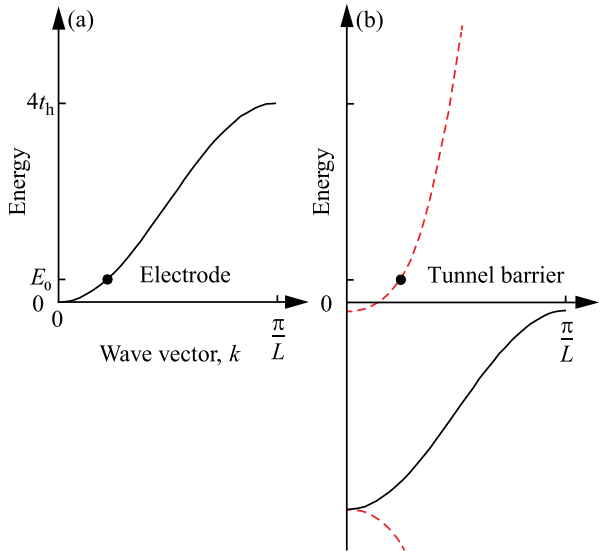

Fig. 8. (a) A propagating electron state (dot) of energy E_0 in the real nearest-neighbor tight-binding cosine band of the electrode (black curve). Energy E_0 is near the conduction band minimum and dispersion has the usual positive curvature. (b) Cosine band shifted down in energy relative to (a) to access states associated with a tunnel barrier. An electron of energy E_0 incident on the barrier may be viewed as tunneling via the k-state (dot) in the complex part of the band structure (red dash curve). (For interpretation of the references to color in this figure legend, the reader is referred to the web version of this article.)

Adopting the simplest nearest-neighbor tight-binding model of atom s-orbitals on a 1D lattice and using complex band structure as a guide, the peak probability of an electron pulse transmitted through a tunnel barrier can be engineered to arrive *before or after* and have a group velocity that is *greater or less* than a pulse propagating in the absence of the barrier. The physics determining this behavior is that of a k-space filter created by the presence of the tunnel barrier. The parameters that control energy eigenvalue as a function of imaginary k-vector in a single-band nearest neighbor tight-binding approximation with atom s-orbitals are t_h, V_B, and L. They determine the slope and curvature of the imaginary band associated with tunneling near the expectation energy of the incident electron. More involved k-space filter behavior can be created by including additional degrees of freedom such as a next-nearest neighbor hopping term, atom p-orbitals, a multi-atom basis per unit cell, and spatial variation of onsite potential U_j within the tunnel barrier. The availability of these and other resources expands the design space for nanoscale electron device applications.

There are potential applications of complex band structure. For example, it improves the peak-to-valley ratio of double-barrier resonant tunnel devices. This is because a tunnel barrier whose imaginary k-vector increases with energy (as shown in Fig. 8(b)) will suppress tunneling at energies greater than the resonant energy.

While the scattering dynamics of wave packets have previously been simulated and characterized both in the continuum [2,11,12] and on 1D lattices [7,13], our approach has been to focus on a minimalist model that captures the key physics. We have not addressed the more detailed complex band structure of actual materials and devices [14]. Also missing are complications due to electron scattering in three dimensions, electron scattering in the presence of other electrons and lattice vibrations, and other many-body interactions. In addition, we have not explored self-consistent calculations of electron current through a device structure. These and other more sophisticated phenomena have been avoided, allowing us to focus on the physics underlying the k-space filter due to the presence of a tunnel barrier.

Finally, we note that superluminal transport of information may not be inferred from Fig. 5(b). A proper comparison of single-bit information detection requires use of a common bit-detection threshold.

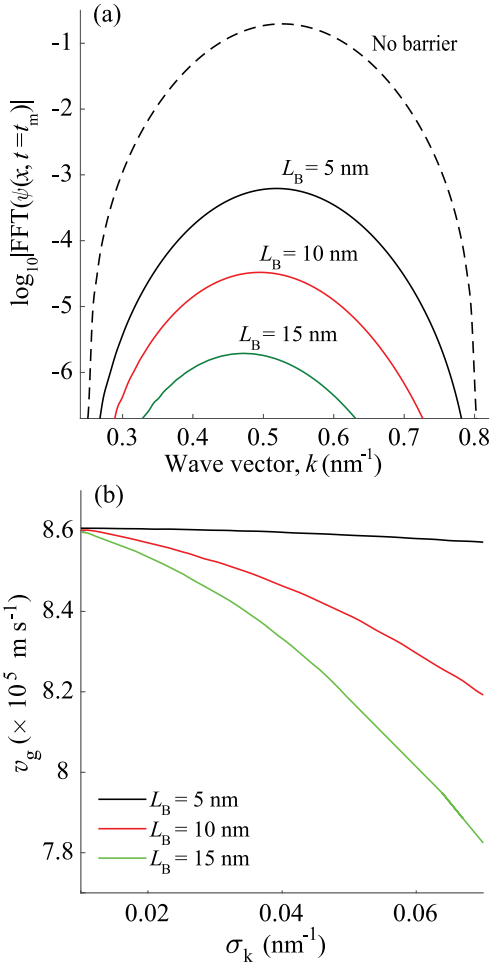

Fig. 9. (a) An incident electron pulse of expectation energy E_0 has a distribution of k-space amplitudes with standard deviation $\sigma_k = 0.07$ nm^{-1} centered on wave vector $k_0 = 0.527$ nm^{-1}. The tunnel barrier acts as a low-pass filter for wave vector amplitudes. The transmitted pulse measured at a time $t_m > 0.94$ ps is distorted relative to the incident pulse, contains k-states with amplitudes that peak at a value $k' < k_0$, and has a group velocity that is less than that of the incident pulse. For barrier thicknesses $L_B = 5$, 10, and 15 nm, $k' = 0.519$, 0.495, and 0.472 nm^{-1} respectively. (b) Group velocity of the transmitted pulse depends on the value of σ_k and L_B. Parameters are as in Fig. 3(a) with $V_B = -0.05 - 4t_h = -8.759$ eV.

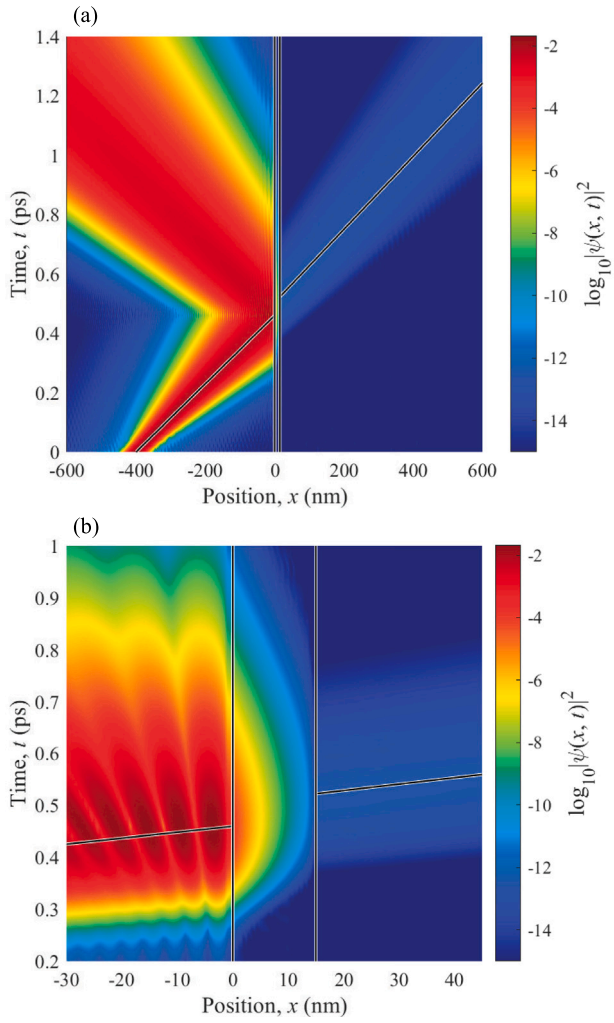

Fig. 10. (a) Spatio-temporal plot of electron probability $|\psi(x,t)|^2$ describing a pulse propagating on a lattice incident on a tunnel barrier with on-site energy V_B. Vertical lines indicate the left and right boundaries of the tunnel barrier. After transmission through the barrier the electron wave packet has a group velocity that is less than that of the pulse propagating in the absence of the barrier. The peak in the attenuated transmitted pulse probability arrives *after* the peak of the pulse propagating in the absence of the tunnel barrier. (b) Detail of (a). Parameters are as in Fig. 9 with $L_B = 15$ nm.

This results in the single-bit tunnel-transmitted arrival information in the pulse occurring on average after that of the pulse with no barrier present. Collision lifetime and the related tunneling time can also be defined by considering such information transport.

5. Conclusion

Complex band structure due to the periodic potential of a crystal can be used to help explain the behavior of single-electron wave-packet tunneling. A nearest-neighbor tight-binding model of atom s-orbitals on a 1D lattice may be used to illustrate the essential physics. The band structure of real k-states in an electrode controls dispersion of a propagating electron pulse. The imaginary component of k-states that are solutions to the Schrödinger equation in a tunnel barrier determine electron wave packet tunneling. The imaginary k-space values in a tunnel barrier may be viewed as a filter that controls the average arrival time, shape, and group velocity of a transmitted single-electron wave packet. Relative to the incident pulse, this k-space filter can be designed using complex band structure as a guide to either increase or decrease the group velocity of the transmitted pulse. It can also be designed so that the average transmitted peak-pulse arrival time occurs before or after that of an electron wave packet propagating in the absence of the tunnel barrier.

CRediT authorship contribution statement

Walter Unglaub: Methodology, Software, Formal analysis, Investigation, Data curation, Writing – original draft, Writing – review & editing, Visualization. **A.F.J. Levi:** Conceptualization, Resources, Writing – original draft, Writing – review & editing, Visualization, Project administration.

Declaration of competing interest

The authors declare that they have no known competing financial interests or personal relationships that could have appeared to influence the work reported in this paper.

Data availability

No data was used for the research described in the article.

Appendix A. Numerical diagonalization

As described in Section 2, the numerical results presented in this paper are calculated by diagonalizing a Hamiltonian matrix whose elements correspond to the allowed transitions between the lattice site basis states [7].

Specifically, the kinetic energy term $-t_h$ populates all matrix elements corresponding to nearest-neighbor transitions from the excitation on node j to $j+1$ such that $\langle j+1|\hat{H}|j\rangle = -t_h$, as well as their hermitian adjoints corresponding to transitions from node $j+1$ to j, such that $\langle j|\hat{H}|j+1\rangle = -t_h$.

The diagonal matrix elements $\langle j|\hat{H}|j\rangle = U_j$ correspond to the onsite energy. These are set to zero everywhere except for lattice sites where the rectangular barrier is placed, in which case the value of $V_B = 0.35$ eV is used. The number of consecutive sites with non-zero energy, N_V, is computed by dividing the barrier thickness L_B by the lattice spacing constant L, so $N_V = L_B/L$.

Finally, since the 1D lattice is periodic, the off-diagonal corner matrix elements must be non-zero, corresponding to hopping allowed from one end of the lattice to the other, and vice versa. Thus, for a 1D lattice with N total sites, $\langle 1|\hat{H}|N\rangle = \langle N|\hat{H}|1\rangle = -t_h$.

Appendix B. Effective hopping energy calculation

Electron effective mass is defined as

$$m_e^* = \frac{\hbar^2}{\frac{d^2E}{dk^2}}. \tag{B.1}$$

Using the expression for nearest-neighbor energy dispersion as measured from the bottom of the s-orbital band, $E = 2t_h(1-\cos(kL))$, we have

$$m_e^* = \frac{\hbar^2}{2t_h\cos(kL)L^2} = \frac{\hbar^2}{(2t_h - E)L^2}, \tag{B.2}$$

where we substitute $2t_h\cos(kL) = 2t_h - E$. Solving for t_h and removing the reference energy term $E/2$, we derive the effective hopping energy for the kinetic energy term in terms of the effective mass and lattice spacing,

$$t_h = \frac{\hbar^2}{2m_e^*L^2}. \tag{B.3}$$

For a given center wave packet energy E_0, we can use this result to calculate the central wave number k_0 so that

$$k_0 = \frac{1}{L}\cos^{-1}\left(1 - \frac{E_0}{2t_h}\right). \tag{B.4}$$

Thus, for an effective mass coefficient $m_e^*/m_0 = 0.07$ and lattice spacing $L = 0.5$ nm, the hopping rate energy $t_h = 2.178$ eV, and therefore $k_0 = 0.527$ nm^{-1} for a center wave packet energy $E_0 = 0.15$ eV.

Appendix C. Predistortion of initialized wave packet

In preparing a single electron wave packet to propagate on a 1D lattice, we began by considering a Gaussian envelope for the pulse. While a pure Gaussian has an infinite domain in the continuum, any waveform defined on a discrete lattice with constant uniform spacing $L = 0.5$ nm is bounded by the maximum wavenumber, $k_{max} = \pi/L$. A Gaussian pulse will have wave vectors with corresponding energies exceeding the barrier energy $V_B = 0.35$ eV. Including these components results in above-barrier scattering and therefore a poorly-defined transmitted pulse peak. In the interest of emphasizing how the filtering action of the rectangular tunnel barrier modifies pulse transmission, we apply a raised cosine filter $\Theta(k)$ to the initialized Gaussian wave packet,

$$\Theta(k) = \begin{cases} \frac{1}{2}\left[1 + \cos\left(\theta(k-k_0)\right)\right], \\ \quad \text{if } |k-k_0| \le k_0 + \eta\sigma_k; \\ 0, \text{ otherwise.} \end{cases} \tag{C.1}$$

In Eq. (C.1), $\theta = \pi/(\eta\sigma_k)$ where η is the limit multiple of standard deviations in k-space comprising the wave packet. Once the hopping term t_h is computed, the limit multiple can be calculated as a function of the barrier energy by algebraically solving the inequality $E(\eta) < V_B$, yielding

$$\eta < \frac{1}{\sigma_k}\left[\frac{1}{L}\cos\left(1 - \frac{V_B}{2t_h}\right) - k_0\right]. \tag{C.2}$$

For the results presented, we take the FFT of the initialized wave packet and apply a raised cosine filter to restrict wave vectors such that the electron has energy components that are less than the tunnel barrier energy. The allowed wave vectors are restricted by setting $\eta = 3.94$ for a central wave vector $k_0 = 0.527$ nm^{-1}. The corresponding energy components in the pulse are bounded by a minimum and maximum energy, E_{min} and E_{max}, respectively.

The raised cosine filter is applied by first taking the FFT of the initialized Gaussian wave packet in real space and then multiplying the resulting wave packet in k-space, $\psi_0(k)$, with the filter $\Theta(k)$ for each value of k, resulting in the distorted wave packet $\psi(k)$ shown in Fig. 11.

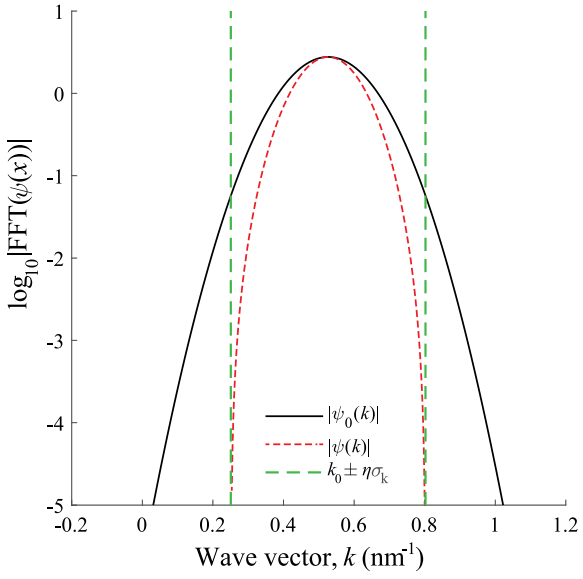

Fig. 11. Initial Gaussian wave packet $|\psi_0(k)|$. Wave packet $|\psi(k)|$ after application of a raised cosine filter to restrict wave vectors such that the electron has energy components that are less than the tunnel barrier energy. For the numerical results shown, we allow all wave vectors within the range $k_0 \pm 3.94\,\sigma_k$. Dashed (green) vertical lines represent the wave vector cutoff values. Parameters are as in Fig. 3. (For interpretation of the references to color in this figure legend, the reader is referred to the web version of this article.)

Finally, we take the inverse Fourier transform of the resulting wave packet to obtain our initial wave packet $\psi(x, t = 0)$ with k-components whose energies do not exceed the tunnel barrier energy. This wave packet is then propagated by unitarily evolving each lattice site amplitude in time.

Appendix D. Calculating k-space representation of transmitted pulse

To calculate the k-space representation of the wave function to the right of the tunnel barrier as shown in Figs. 4 and 9, we first require the system to evolve sufficiently long so that a pulse is transmitted and characterized by a pulse propagating to the right of the tunnel barrier with a well-defined peak. We then examine the magnitude of the wave function to the right of the barrier and select at least two criteria which must be met. Firstly, enough spatial points (nodes) must be sampled in order to properly resolve $\psi(k)$. Secondly, we require that the leading and trailing edges of the transmitted pulse magnitude must

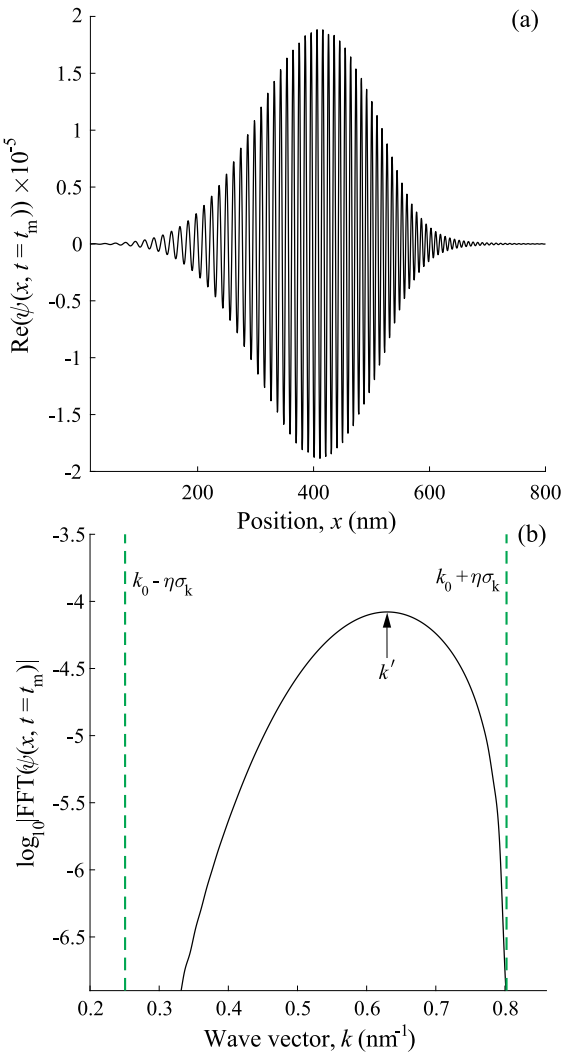

Fig. 12. (a) Transmitted pulse $\mathrm{Re}(\psi(x > x_R, t_m))$ measured at time $t_m = 0.78$ ps with peak pulse magnitude $|\psi(x_R, t_m)|$ at $x_R = 407.5$ nm. (b) FFT of the wave function $\psi(x, t_m)$ for $x > L_B$. Transmission through the tunnel barrier distorts the distribution of k-space amplitudes. There is a bias toward higher values of wave vector with a peak at $k' = 0.630\ \mathrm{nm}^{-1} > k_0 = 0.527\ \mathrm{nm}^{-1}$. Parameters are as in Fig. 3, with $\eta = 3.94$.

be less than one part per thousand of the transmitted peak value, such that the resulting numerical values for $|\psi(k)|$ do not vary significantly as the transmitted pulse continues to propagate to the right of the barrier. This requires a sufficiently large spatial domain to the right of the tunnel barrier. For all figures in this paper, we set the right boundary of the domain at $x_{\mathrm{right}} = 800$ nm to satisfy these conditions for the set of parameters as listed in Fig. 5.

We automate calculation of the measurement time t_m by selecting the transmitted peak measurement position x_R to be halfway between the right edge of the tunnel barrier ($x = L_B$) and the right edge of the spatial domain ($x = x_{\mathrm{right}}$), so that $x_R \equiv (x_{\mathrm{right}} - L_B)/2$. From this, the measurement time t_m is defined as the time when the transmitted pulse peak arrives at the lattice node positioned at x_R. As exemplified in Fig. 12, the transmitted pulse is well-defined to the right of the barrier, from which the FFT may be computed.

References

[1] R. Landauer, Th. Martin, see For example, Barrier interaction time in tunneling, Rev. Modern Phys. 66 (1994) 217–228;
H.G. Winful, Tunneling time, the hartman effect, and superluminality: a proposed resolution of an old paradox, Phys. Rep. 436 (2006) 1–69;
R. Ramos, D. Spierings, I. Racicot, A.M. Steinberg, Measurement of the time spent by a tunnelling atom within the barrier region, Nature 583 (2020) 529–532;
T. Rivlin, E. Pollak, R.S. Dumont, Determination of the tunneling flight time as the reflected phase time, Phys. Rev. A 103 (2021) 012225.

[2] K. Jensen, J. Lebowitz, J. Riga, D. Shiffler, R. Seviour, Wigner wave packets: Transmission, reflection, and tunneling, Phys. Rev. B 103 (2021) 155427.

[3] M. Razavy, Quantum Theory of Tunneling, second ed., World Scientific Publishing Company, 2014.

[4] Y. Yin, Z. Zhang, C. Shao, J. Robertson, Y. Guo, Computational study of transition metal dichalcogenide cold source MOSFETs with sub-60 mV per decade and negative differential resistance effect, Npj 2D Mat. Appl. 6 (2022) 55.

[5] E. Sasıoglu, I. Mertig, Theoretical prediction of semiconductor-free negative differential resistance tunnel diodes with high peak-to-valley current ratios based on two-dimensional cold metals, ACS Appl. Nano Mat. 6 (2023) 3758.

[6] C.G. Darwin, Free motion in the wave mechanics, Proc. R. Soc. Lond. Ser. A Math. Phys. Eng. Sci. 117 (1928) 258–293.

[7] M. Staelens, F. Marsiglio, Scattering problems via real-time wave packet scattering, Amer. J. Phys. 89 (2021) 693–701.

[8] M.G. Reuter, see For a review, A unified perspective of complex band structure: interpretations, formulations, and applications, J. Phys.: Condens. Matter 29 (2017) 053001.

[9] T.E. Hartman, Tunneling of a wave packet, J. Appl. Phys. 33 (1962) 3427–3433.

[10] F.T. Smith, Lifetime matrix in collision theory, Phys. Rev. 118 (1960) 349–356.

[11] K. Smith, G. Blaylock, Simulations in quantum tunneling, Amer. J. Phys. 85 (2017) 763–768.

[12] T.A. Saxton, A.L. Harris, Control of arrival time using structured wave packets, Phys. Lett. A 388 (2020) 127038.

[13] W. Kim, L. Covaci, F. Marsiglio, Impurity scattering of wave packets on a lattice, Phys. Rev. B 74 (2006) 205120.

[14] N.F. Hinsche, M. Fechner, P. Bose, S. Ostanin, J. Henk, I. Mertig, P. Zahn, For example, Strong influence of complex band structure on tunneling electroresistance: A combined model and ab initio study, Phys. Rev. B 82 (2010) 214110.